Biochemical and Biophysical Research Communications 456 (2015) 392–397

Contents lists available at ScienceDirect

Biochemical and Biophysical Research Communications

journal homepage: www.elsevier.com/locate/ybbrc

Three-dimensional human arterial wall models for *in vitro* permeability assessment of drug and nanocarriers

Paninee Chetprayoon, Michiya Matsusaki, Mitsuru Akashi *

Department of Applied Chemistry, Graduate School of Engineering, Osaka University, 2-1 Yamadaoka, Suita 565-0871, Osaka, Japan

ARTICLE INFO

Article history:
Received 27 October 2014
Available online 2 December 2014

Keywords:
Arterial wall model
3D-tissue
Permeability assay
Dextran
Poly(γ-Glutamic Acid)
Nanoparticles

ABSTRACT

Monolayers of endothelial cells (1L-ECs) have been generally used as *in vitro* vascular wall models to study the vascular mechanisms and transport of substances. However, these two-dimensional (2D-) system cannot represent the properties of native vascular walls which have a 3D-structure and are composed of not only ECs, but also smooth muscle cells (SMCs) and other surrounding tissues. Here in, 5-layered (5L) 3D-arterial wall models (5L-AWMs) composed of EC monolayer and 4-layered SMCs were constructed by hierarchical cell manipulation. We applied the 5L-AWMs to evaluate their barrier function and permeability to nano-materials in order to analyze drug, or drug nanocarrier permeability to the blood vessel *in vitro*. Barrier property of the 3D-AWMs was confirmed by Zonula occludens (ZO-1) staining and their transendothelial electrical resistance (TEER), which was comparable to 1L-ECs, while the SMCs showed close to zero. The effect of substance size to permeability across the 5L-AWMs was clearly observed from dextrans with various molecular weights, which agreed well with the known phenomena of the *in vivo* blood vessels. Importantly, transport of nano-materials could be observed across the depth of 5L-AWMs, suggesting the advantage of 3D-AWMs over general 2D-systems. By using this system, we evaluate the transport of 35 nm phenylalanine-modified poly(γ-Glutamic Acid) nanoparticles (γ-PGA-Phe NPs) as a candidate of biodegradable drug carrier. Interestingly, despite of having comparable size to dextran-2000k (28 nm), the γ-PGA-Phe NPs distinctly showed approximately 20 times faster transport across the 5L-AWMs, suggesting the effect of intrinsic properties of the substance on the transport. This *in vitro* evaluation system using the 3D-AWMs is therefore useful for the design and development of nano-drug carriers for treatment of vascular diseases, such as atherosclerosis.

1. Introduction

One of the difficulties in the development of drug delivery nanocarriers is the lack of an *in vitro* system which can represent the conditions of the *in vivo* native tissues. Generally, in the study of vascular diseases or the development of drug carriers, monolayer culture of vascular endothelial cells (ECs), or either coculture model of vascular ECs and vascular smooth muscle cells (SMCs) which are cultured on both sides of culture membrane, are used as an *in vitro* model to study the response of cells to drugs or nanomaterials [1,2]. Studies of, such as targeting of specific ligand molecules, or the response to cytokines produced from both cells, are possible to study from these coculture models [3,4]. Nevertheless, since both types of cells do not directly contact each other, these coculture models cannot replicate the complex interactions between ECs and SMCs, or with the extracellular matrix including surrounding tissues. More importantly, the transport or the permeability of substances across the depth of vascular wall cannot be evaluated in these two-dimensional (2D-) systems since there are composed of only one or two layers of cells. There are some report of 3D-coculture model of ECs and SMCs by forming spheroids [5]. Spheroid system can provide direct interactions between ECs and SMCs, however, not suitable for study of the permeability of drugs or drug carriers due to the inability to control the layer number of SMCs. An *in vitro* 3D-model of arterial wall is therefore desired for the development of drug carriers.

We have reported a novel hierarchical cell manipulation technique by fabrication of nanometer-sized layer-by-layer (LbL) films composed of fibronectin (FN) and gelatin (G) onto the cell membrane [6]. This technique enables us to construct 3D-multilayered tissues with controllable cell types and layer number. Recently, we have reported the construction and characterization of 3D-arterial wall models (AWMs) by hierarchical cell manipulation [7], and the diffusion of nitric oxide could be analyzed in the 3D-AWMs [8]. The aim of this study is to develop a new method for evaluation of the

* Corresponding author. Fax: +81 6 6879 7359.
E-mail address: akashi@chem.eng.osaka-u.ac.jp (M. Akashi).

http://dx.doi.org/10.1016/j.bbrc.2014.11.094
0006-291X/

permeability and transport of drugs or drug carriers by using the 3D-human vascular wall models consisted of a layer of ECs and 4 layers of SMCs for the development of drug delivery systems (DDS) (Fig. 1A). Herein, we demonstrate the effect of size, and transport pathway of substances on their permeability across the arterial wall by using the 3D-AWMs. The response of 3D-AWMs to an inflammatory cytokine, as well as the effect on their permeability property was also investigated. The 3D-AWMs will allow us to better understand the interaction of materials with the arterial wall, and appropriate physical properties, such as size, component, and surface property of the drug carrier which affect the permeability across the arterial walls for the development of drug carriers.

2. Materials and methods

2.1. Construction of 5L-AWMs by hierarchical cell manipulation

Umbilical artery smooth muscle cells (UASMCs) (Cambrex, USA) at passage 7–10 were cultured in smooth muscle basal medium (SmBM; Cambrex, USA) containing hEGF, hFGF-B, GA-1000, 5% fetal bovine serum (FBS) and insulin. Human umbilical vein endothelial cells (HUVECs) at passage 7–10 were cultured in endothelial basal medium-2 (EBM-2; Cambrex, USA) containing hydrocortisone, hFGF-B, VEGF, R3-IGF-1, ascorbic acid, 5% FBS, hEGF and GA-1000. The 3D-AWMs were constructed by hierarchical cell manipulation following the previous report with some modifications [7]. The 3D-AWMs were constructed on polyester membrane inserts (pore size 0.4 μm) (Corning, USA), and cultured in a 24-well culture plate. 6.7×10^4 SMCs were seeded onto FN (Sigma Aldrich, USA)-coated inserts to be a first layer. After being cultured for more than 8 h, monolayered SMCs were rinsed with Tris–HCl solution. FN-G nanofilms were fabricated on the cells by alternately immersing cells in 0.04 mg/mL solution of FN and G (Wako, Japan) for totally 9 steps, and rinsing with Tris–HCl solution after each step. SMCs with similar cell number were seeded onto the FN-G-coated monolayer of SMCs to be a second layer, and cultured for more than 8 h. The process was repeated until the construction of 4L-SMC was completed. The top layer of ECs were applied by the same procedure to obtain 1L-EC/4L-SMC (5L-AWMs). Culture medium in the inserts was changed to 0.3 mL of EBM-2 after construction of the EC layer, while the medium in the culture wells was 1 mL SmBM. Cell culture was maintained in 5% CO_2 at 37 °C.

2.2. Synthesis of phenylalanine-modified poly(γ-Glutamic Acid) (γ-PGA-Phe)copolymer and preparation of γ-PGA-Phe NPs

The γ-PGA-Phe copolymer (grafting degree of 65%) was synthesized according to the reported method [9]. Alexa Fluor 488 (Alexa488; Molecular Probe, USA)-labeled γ-PGA-Phe nanoparticles (NPs) with size of 35 nm [10] were used in the visualization of transport of substance across the 5L-AWMs.

2.3. Permeability assessment

Fluorescein isothiocyanate (FITC)-labeled dextrans (Sigma Aldrich, USA) with various molecular weights (4k, 70k, 250k, and 2000k), FITC-labeled bovine serum albumin (BSA; Sigma Aldrich, USA), and Alexa488-labeled γ-PGA-Phe NPs were used in the permeability experiment. The substances were dissolved in phosphate buffered saline (PBS) solution (5 mg/mL) and diluted in EBM-2 culture medium to 1 mg/mL. After construction of 5L-AWMs and cultured for 1 day, culture medium in the culture well (lower chamber) was refreshed with 1 mL fresh culture medium, and culture medium in the culture insert was replaced with 200 μL EBM-2 containing the substances. The 5L-AWMs were kept in the cell culture incubator (37 °C) throughout the experiment. 30 μL sample was collected from medium in the lower chamber to evaluate the concentration of permeated substances at each time point. Similar volume of fresh culture medium was added to the lower

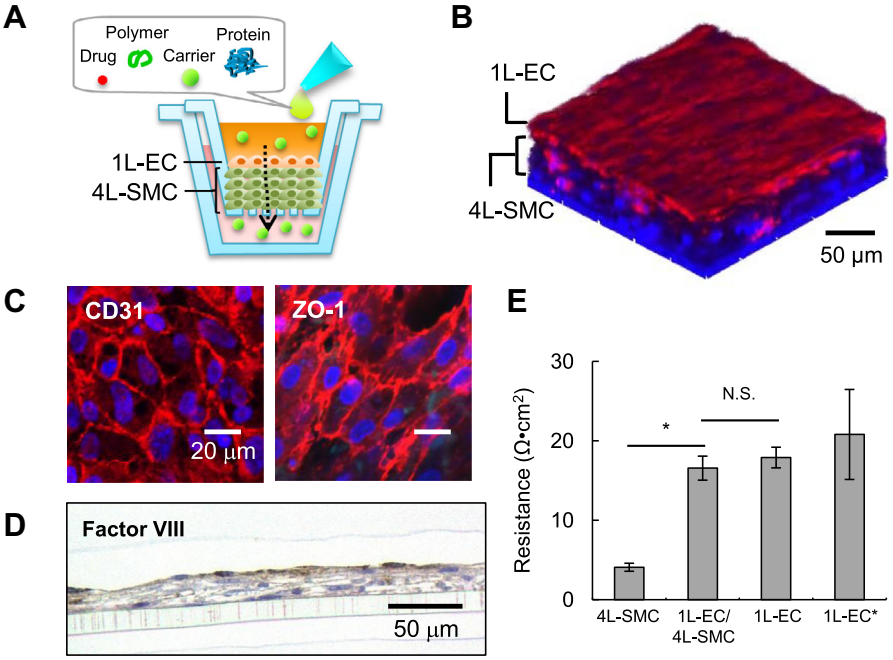

Fig. 1. Characterizations of structure and barrier properties of 3D-AWMs. (A) Illustration showing the evaluation of nanomaterial permeability across the 3D-structure of AWMs. (B) 3D-reconstructed image of 5L-AWM (1L-EC/4L-SMC) taken by CLSM, ECs were stained with CD31 (red) and nuclei were stained with DAPI (blue). (C) Immunostaining of ECs (red) in 3D-AWM; membrane marker (CD31), and tight junction (ZO-1) (D) Histological cross-section of 5L-AWM; ECs were stained with factor VIII (brown). (E) TEER of 5L-AWM compared to 4L-SMC and 1L-EC *[11–14]. Error bars represent standard deviation of $n \geqslant 3$. $^*p < 0.01$ (Student's *t*-test). (For interpretation of the references to color in this figure legend, the reader is referred to the web version of this article.)

chamber after the sample was collected each time to maintain the volume. The concentration of permeated substances was determined by measurement of fluorescence intensity using NanoDrop 3300 Fluorospectrometer (Thermo Scientific, USA). Permeability was evaluated in % as compared to total amount of substance added.

To investigate the effect of cellular uptake on permeability, permeability of 5L-AWMs was evaluated at 4 °C to lower the energy-dependent endocytosis. The 5L-AWMs were pre-incubated at 4 °C on an ice bath for 40 min before starting the experiment, and maintained at 4 °C throughout the permeability experiment.

2.4. Tumor necrosis factor alpha (TNF-α) treatment

For the study of response to inflammatory cytokine, 5L-AWMs or EC monolayers (1L-ECs) were incubated in culture medium containing TNF-α with concentration varied from 0 to 100 ng/mL for 4 h prior to permeability test. The medium containing TNF-α was then removed and the cells were washed with PBS solution before starting the permeability experiment.

2.5. Transendothelial electrical resistance (TEER) measurement of 5L-AWMs

The culture media in culture insert and culture well were replaced with PBS solution. The TEER values of 5L-AWMs, 4L-SMCs, and 1L-ECs were measured by Millicell ERS-2 Voltohmmeter (Merck Millipore, Germany).

2.6. Time-lapse visualization of transport of materials across the 3D-AWMs

The 5L-AWMs were labeled with cell tracker red after construction. FITC-labeled dextran-4k, dextran-2000k, and 35 nm γ-PGA-Phe NPs were used to observe their transport across the 5L-AWMs. The 5L-AWM in a culture insert was placed on a 35-mm glass-bottom dish (Wako, Japan) filled with SmBM culture medium, and placed in a sample holder of a confocal laser scanning microscopy (CLSM; FLUOVIEW FV10i, Olympus, Japan). The culture insert was fixed to the glass-bottom dish by an adhesive tape to maintain its position before and after adding dextran or γ-PGA-Phe NPs. Z-stack images of 5L-AWMs were taken in a time-lapse mode during 24 h of permeability. Transport of substances to the bottom layer of 5L-AWMs was determined from the area of threshold green fluorescence using MetaMorph software.

2.7. Fluorescence imaging of immunostained 3D-AWMs

UASMCs in 5L-AWMs were stained with cell tracker red. HUVECs were immunostained with anti-human-CD31 (Dako, Denmark) or anti-human-Zonula occludens (ZO-1; Dako, Denmark) antibody. Briefly, 3D-AWMs were permeabilized with 0.2% Triton-X for 15 min and blocked with 1% BSA/PBS for 1 h. The tissues were then incubated with the primary antibodies (1:50) for 1 h. After a washing step, the secondary antibodies (1:200) were added to the tissues. The tissues were finally incubated in diamidino-2-phenylindole (DAPI) (1:1000) for 20 min to stain their nuclei. The tissues were observed by CLSM.

3. Results and discussion

3.1. Characterization of structures and barrier functions of 3D-AWM

The structure of 5L-AWM was observed by CLSM. The CLSM images revealed the layered structure of 5L-AWM, with a top layer of ECs (Fig. 1B). ECs were immunostained with CD-31 and ZO-1 to understand the structure of the EC layer with a presence of tight junction proteins (Fig. 1C). The thickness of 5L-AWM was evaluated from the hematoxylin and eosin (H&E)-stained cross section and was approximately 30 μm. The histology of 5L-AWM showed approximately a 5-layered structure as revealed by the alignment of their nuclei, and a top layer of ECs which were stained with factor VIII (Fig. 1D).

To evaluate the barrier function which is an important property of the vascular wall, TEER was measured from the 5L-AWMs and 1L-EC (Fig. 1E). Since the TEER value varies depending on the type and source of cells, we compared the TEER of 1L-EC in our study with the values reported in other studies. The TEER of 5L-AWMs was 17 Ωcm^2, which was comparable to, but slightly lower than that of 1L-EC in this study and other studies [11–14]. This is probably because the EC layer was cultured on layers of SMCs, unlike the 1L-EC which was grown on a polyester culture membrane and formed a compact monolayer. On the other hand, the TEER of 4L-SMC without EC layer was close to zero due to the lack of barrier property of SMCs, indicating the importance of EC layer in barrier property. Hence, the 5L-AWMs have barrier property and are expected to be useful as an *in vitro* 3D-vascular model.

3.2. Tolerance of 3D-AWMs to inflammatory cytokine

Because of the presence of 3D-structure, the response of cells to chemicals or cytokines is different from 2D-monolayer. General examples can be found in many tumor spheroids that show resistance to drugs, which effectively works in monolayer cultured tumor cells [15]. The interactions between ECs and SMCs in the 3D-structure also affect the uptake of low-density lipoproteins (LDL) in response to shear stress, so that the coculture of ECs and SMCs became more tolerance to the shear stress [16]. In our 5L-AWMs, we evaluated the effect of TNF-α, an inflammatory cytokine known to cause loosening of EC intercellular junctions, thus increasing the permeability of EC layer [17], to the barrier function of 5L-AWMs by TEER measurement. In the 1L-ECs, after incubating with TNF-α for 4 h and removal, the TEER became apparently lower after performing permeability test with dextran-70k for 24 h, while the TEER of the 1L-EC that did not undergo the permeability test was not different from the non-treated cells (Fig. 2A). On the other hand, the 5L-AWMs did not show an obvious decreasing of TEER after TNF-α and permeability test (Fig. 2B). These results show the tolerance of the 5L-AWM to inflammatory cytokine and stability of barrier function after being permeated with non-specific substance, as compared to 1L-EC. Similar phenomena was also reported in bilayer culture of ECs and SMCs where resistance to inflammatory cytokines was shown [18]. However, increasing the TNF-α concentration did not appear to lower the TEER after 4 h incubation in either cases.

Permeability to dextran-70k was evaluated in non-treated and TNF-α-treated 5L-AWMs, 1L-ECs, and 4L-SMCs (Fig. 2C). The permeability in 5L-AWMs slightly increased from 12.1% to 15% when treated with TNF-α. On the other hand, the permeability in 1L-ECs increased from 3.8% to 6.4%. The higher permeability of 5L-AWMs as compared to 1L-ECs is probably because the EC layer in 5L-AWMs was cultured on layers of SMCs, which has a rough surface, unlike the 1L-EC which was grown on a flat polyester culture membrane and formed a more compact monolayer. More importantly, there has been reported that ECs and SMCs affect each other's functions when cocultured together. Higher permeability to LDL was observed in the coculture of ECs and SMCs on each side of the culture membrane, as compared to 1L-EC [19]. Nevertheless, we had observed that the 3D-AWMs showed smaller increase in permeability after TNF-α treatment as compared to 1L-EC, thus agreed well with their smaller change in TEER. On the other hand,

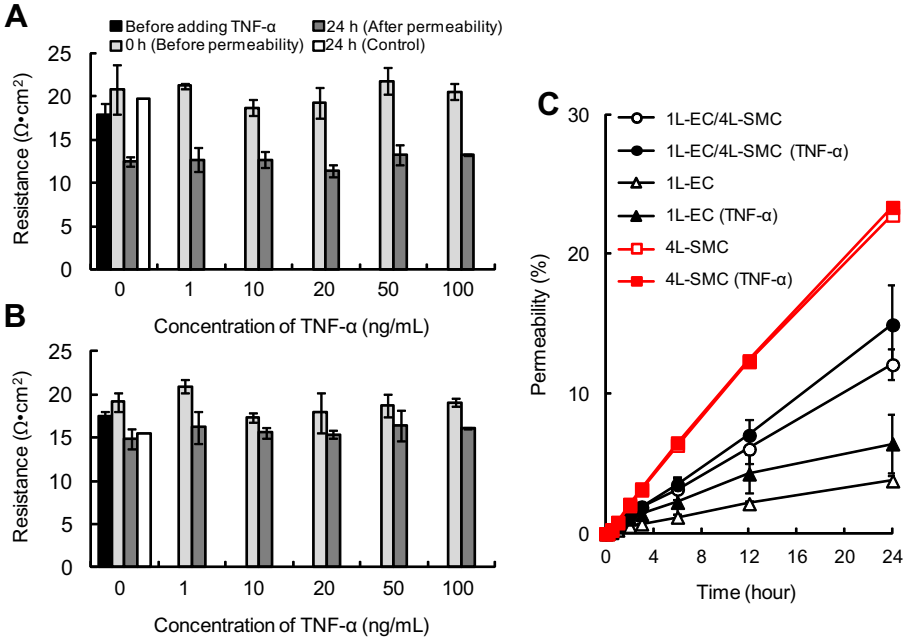

Fig. 2. Tolerance to TNF-α of 5L-AWM as compared to 1L-EC. TEER of (A) 1L-EC, and (B) 5L-AWMs before and after incubating with TNF-α for 4 h and removal (0 h), and permeability tested with dextran-70k for 24 h, the control is cells without permeability test. Error bars represent standard deviation of $n \geqslant 2$. (C) Effect of TNF-α (10 ng/mL) to permeability of dextran-70k across the 3D-AWM, 1L-EC, and 4L-SMC. Error bars represent standard deviation of $n \geqslant 3$.

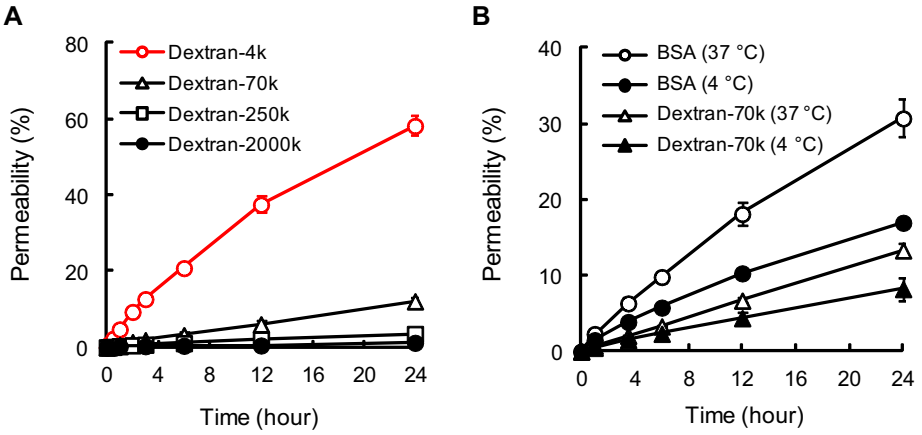

Fig. 3. Permeability property of the 5L-AWM (A) The effect of size on permeability of the 5L-AWM evaluated with FITC-dextran with various molecular weights. Dextran-4k was highlighted in red to indicate the permeable size across the 5L-AWMs ($n = 3$). (B) The effect of cellular uptake on permeability of the 5L-AWMs evaluated with BSA, as compared to dextran-70k, at 37 °C and 4 °C. Error bars represent standard deviation of $n = 3$. (For interpretation of the references to color in this figure legend, the reader is referred to the web version of this article.)

4L-SMC showed no different permeability after treatment with TNF-α, which was due to the lack of EC layer. Therefore, 4L-SMCs showed higher permeability to dextran-70k.

3.3. Effect of substance size to permeability of 3D-AWMs

The barrier property of 5L-AWMs was revealed from the staining of tight junction protein; ZO-1, and TEER measurement. Next, we evaluated the permeability function of the 5L-AWMs by using FITC-labeled dextran as a drug model. Dextrans with molecular weights (MW) of 4k, 70k, 250k, and 2000kDa, corresponding to size of less than 2 nm, 6 nm, 11 nm, and 28 nm [20], respectively, were used to understand the effect of size on the permeability of the 5L-AWMs. The permeability of dextran clearly showed a size-dependent manner, which the permeability to dextran-4k, 70k, 250k, and 2000k was 58.2%, 12.1%, 3.5%, and 1.2%, respectively (Fig. 3A). While larger dextrans almost could not permeate across the 5L-AWMs, only dextran-4k showed high permeability. These results indicated directly the effect of size on permeability, which is restricted by the tight junctions of endothelial layer. In a normal vascular wall, only non-specific material which is smaller than 2 nm can permeate across this paracellular pathway [21]. Our 5L-AWMs also showed similar effect of size on permeability as observed in the blood vessels of the mouse [22].

3.4. Effect of transport pathway to permeability of 3D-AWMs

We have demonstrated the permeability of 5L-AWMs by using dextran which is a non-specific materials and permeates via the paracellular pathway through intercellular junctions, and is therefore size restricted. BSA which is known to take a receptor-mediated endocytosis (cellular uptake), or a transcellular pathway

[23], was used to evaluate the effect of transport pathway on permeability across the 5L-AWMs as compared to dextran-70k in this study. Despite having comparable sizes (MW of BSA: 66.5 kDa), the permeability of BSA was distinctly higher than that of dextran-70k at 37 °C, as expected from the effect of transcellular transport (Fig. 3B). Permeability of both BSA and dextran-70k decreased when the experiment was performed at 4 °C to lower the effect of energy-dependent endocytosis [24], thus lowering transcellular transport. The BSA decreased almost by half, from 30.7% to 17%, when the experiment was performed at 4 °C. On the other hand, the permeability of dextran-70k at 37 °C was lower than that of BSA, and slightly decreased from 13.3% to 8.2%. The cellular uptake might not be completely inhibited at 4 °C, and therefore, some transcellular transport of BSA still occurred. This effect of transcellular transport to permeability of BSA was also observed in 1L-EC, which decreased from 20.3% to 11.6% (data not shown). Another study also reported a similar effect using BSA and dextran-70-k to permeate across 1L-EC [25]. Nevertheless, in this system, not only the ECs were present, but there were also SMCs in a 3D-structure. This study demonstrated, for the first time, the permeability and transport pathway in the *in vitro* constructed human 5L-AWM, which is composed entirely of cells without supporting materials.

3.5. Visualization of permeability of dextran and nanoparticles across the 3D-AWMs

With the presence of 3D-structure of the AWMs, it is possible to see the transport of materials across the entire depth of the 5L-AWMs. Dextran-4k was used to observe the diffusion across the structure since it is small enough to be permeable. After adding the culture medium containing dextran-4k to the 5L-AWMs, we observed the bottom layer of 5L-AWMs stained with cell tracker red by CLSM (Fig. 4A). When dextran-4k was added, the green fluorescence of the dextran gradually appeared at the bottom layer as time passed, indicating that the dextran had reached the bottom layer (Supplementary movie S1). The area of the threshold green fluorescence was evaluated from the image of bottom layer during 24 h. When all area of the bottom layer showed green color, we assumed that the layer was saturated with dextran (100%). However, this observation just aids in understanding the permeability, which should be evaluated from the concentration below the culture insert. This time-dependent transport represents the major advantage of 3D-AWMs that enables the analysis of material transport across the entire depth of tissue. This information cannot be obtained in general EC monolayers.

After we successfully observed the transport of dextran-4k across the 5L-AWMs, dextran-2000k and 35 nm γ-PGA-Phe NPs were used to see the effect of different materials with different morphologies, but have comparable sizes. Interestingly, while dextran-2000k slowly appeared at the bottom layer due to its large size, and took almost 20 h (T_{50}) to cover 50% of area of the bottom layer, 35 nm γ-PGA-Phe NPs drastically showed faster transport to the bottom layer and T_{50} was 1 h, 20-time faster than the dextran (Supplementary movies S2 and S3). The results show that morphology or other factors may influence permeability across the vascular wall. Different transport profiles of two different molecules were demonstrated by the 3D-AWMs (Fig. 2c). These types of findings cannot be obtained in the 2D-culture, and are difficult to be evaluated in an *in vivo* model. This knowledge will be very useful for the design and evaluation of a drug carrier for treatment of vascular disease, such as atherosclerosis.

In conclusion, we have established a system of *in vitro* evaluation of nano-material transport across the 3D-AWMs. To the best of our knowledge, this is the first report that evaluated permeability across the 3D-vascular wall model composed entirely of cells. The effect of size to permeability by paracellular pathway was clearly observed in the 3D-AWMs, and agreed well with the *in vivo* findings, suggesting the usefulness of 3D-AWMs. The difference between the 3D-AWM and the 2D-endothelial monolayer is

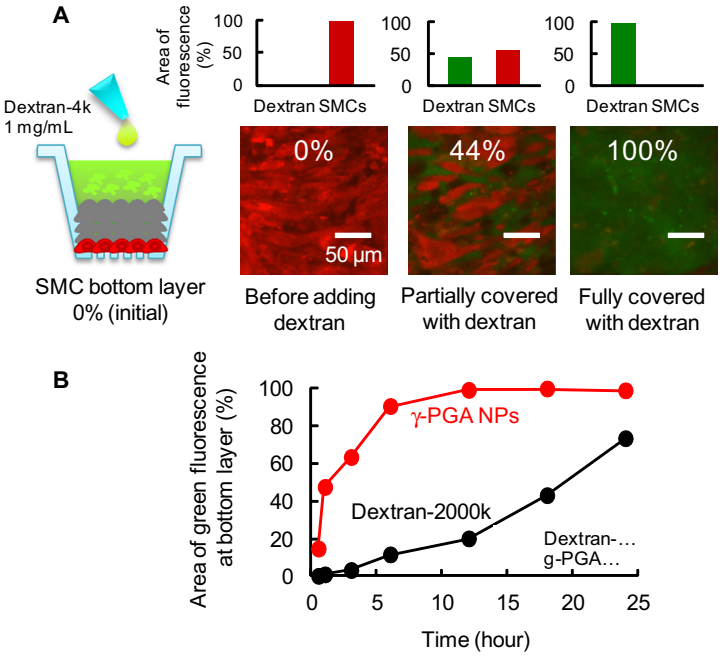

Fig. 4. Visualization of the transport of substances across the 5L-AWMs by time lapse mode of CLSM. (A) The illustration of 5L-AWM in permeability experiment showing the layer of observation highlighted in red. CLSM images of the bottom layer showing percentage of area covered with permeated dextran-4k (green) during the time point, cells were stained with cell tracker (red). (B) Transport of dextran-2000k and γ-PGA-Phe NPs, the graph shows percentage of threshold green area at the bottom layer of 5L-AWM which was covered by fluorescence of the substances during 24 h of incubation. (For interpretation of the references to color in this figure legend, the reader is referred to the web version of this article.)

not only their structures, but also the response to stimuli such as TNF-α, indicating the significance of 3D-tissues. Up to now, most of the studies that evaluate properties of nano-materials to vascular wall have relied on *in vitro* 2D-systems. The 3D-AWMs may represent a vascular wall with property more resemble to the native tissue, and provide useful information for the design and development of drug carriers for treatment of vascular diseases, such as atherosclerosis.

Acknowledgments

This work was supported by the NEXT Program (LR026), a Grant-in-Aid for Scientific Research (S), and the SENTAN-JST Program. We also thanks to Mr. Fumiaki Shima who kindly provided us 35 nm γ-PGA-Phe NPs.

Appendix A. Supplementary data

Supplementary data associated with this article can be found, in the online version, at http://dx.doi.org/10.1016/j.bbrc.2014.11.094.

References

[1] T. Ziegler, R.W. Alexander, R.M. Nerem, An endothelial cell-smooth muscle cell co-culture model for use in the investigation of flow effects on vascular biology, Ann. Biomed. Eng. 23 (1995) 216–225.
[2] S.L. Rose, J.E. Babensee, Complimentary endothelial cell/smooth muscle cell co-culture systems with alternate smooth muscle cell phenotypes, Ann. Biomed. Eng. 35 (2007) 1382–1390.
[3] G. Di Luozzo, J. Bhargava, R.J. Powell, Vascular smooth muscle cell effect on endothelial cell endothelin-1 production, J. Vasc. Surg. 31 (2000) 781–789.
[4] D.I. Axel, R. Riessen, A. Athanasiadis, H. Runge, G. Ko, K.R. Karsch, Growth factor expression of human arterial smooth muscle cells and endothelial cells in a transfilter coculture system, J. Mol. Cell. Cardiol. 29 (1997) 2967–2978.
[5] T. Korff, S. Kimmina, G. Martiny-Baron, H.G. Augustin, Blood vessel maturation in a 3-dimensional spheroidal coculture model: direct contact with smooth muscle cells regulates endothelial cell quiescence and abrogates VEGF responsiveness, FASEB J. 15 (2001) 447–457.
[6] M. Matsusaki, K. Kadowaki, Y. Nakahara, M. Akashi, Fabrication of cellular multilayers with nanometer-sized extracellular matrix films, Angew. Chem. Int. Ed. 46 (2007) 4689–4692.
[7] M. Matsusaki, K. Kadowaki, E. Adachi, T. Sakura, U. Yokoyama, Y. Ishikawa, et al., Morphological and histological evaluations of 3D-layered blood vessel constructs prepared by hierarchical cell manipulation, J. Biomater. Sci. Polym. Ed. 23 (2012) 63–79.
[8] M. Matsusaki, S. Amemori, K. Kadowaki, M. Akashi, Quantitative 3D analysis of nitric oxide diffusion in a 3D artery model using sensor particles, Angew. Chem. Int. Ed. 50 (2011) 1–6.
[9] T. Akagi, T. Kaneko, T. Kida, M. Akashi, Preparation and characterization of biodegradable nanoparticles based on poly(gamma-glutamic acid) with l-phenylalanine as a protein carrier, J. Control. Release 108 (2005) 226–236.
[10] T. Akagi, F. Shima, M. Akashi, Intracellular degradation and distribution of protein-encapsulated amphiphilic poly(amino acid) nanoparticles, Biomaterials 32 (2011) 4959–4967.
[11] S. Imaizumi, T. Kondo, M.A. Deli, G. Gobbel, F. Joó, C.J. Epstein, et al., The influence of oxygen free radicals on the permeability of the monolayer of cultured brain endothelial cells, Neurochem. Int. 29 (1996) 205–211.
[12] T. Horiuchi, K. Matsunaga, M. Banno, Y. Nakano, K. Nishimura, C. Hanzawa, et al., HPMCs induce greater intercellular delocalization of tight junction-associated proteins due to a higher susceptibility to H2O2 compared with HUVECs, Perit. Dial. Int. 29 (2009) 217–226.
[13] R.D. Hurst, J.B. Clark, Alterations in transendothelial electrical resistance by vasoactive agonists and cyclic AMP in a blood–brain barrier model system, Neurochem. Res. 23 (1998) 149–154.
[14] W.K. Sumanasekera, G.U. Sumanasekera, K.A. Mattingly, S.M. Dougherty, R.S. Keynton, C.M. Klinge, Estradiol and dihydrotestosterone regulate endothelial cell barrier function after hypergravity-induced alterations in MAPK activity, Am. J. Physiol. Cell Physiol. 293 (2007) C566–C573.
[15] S. Sakai, K. Inamoto, Y. Liu, S. Tanaka, S. Arii, M. Taya, Multicellular tumor spheroid formation in duplex microcapsules for analysis of chemosensitivity, Cancer Sci. 103 (2012) 549–554.
[16] K. Niwa, T. Kado, J. Sakai, T. Karino, The effects of a shear flow on the uptake of LDL and acetylated LDL by an EC monoculture and an EC-SMC coculture, Ann. Biomed. Eng. 32 (2004) 537–543.
[17] R.J. Stewart, T.S. Kashour, P.A. Marsden, Vascular endothelial platelet endothelial adhesion molecule-1 (PECAM-1) expression is decreased by TNF-alpha and IFN-gamma. Evidence for cytokine-induced destabilization of messenger ribonucleic acid transcripts in bovine endothelial cells, J Immunol. 156 (1996) 1221–1228.
[18] K. Bohlin, I.A. Cotgreave, Pro-inflammatory cytokines increase the permeability of paracetamol across a human endothelial-smooth muscle cell bilayer model, Scand. J. Clin. Lab. Invest. 59 (1999) 239–246.
[19] J. Alexander, R. Miguel, D. Graham, Low density lipoprotein uptake by an endothelial-smooth muscle cell bilayer, J. Vasc. Surg. 13 (1991) 444–451.
[20] J.K. Armstrong, R.B. Wenby, H.J. Meiselman, T.C. Fisher, The hydrodynamic radii of macromolecules and their effect on red blood cell aggregation, Biophys. J. 87 (2004) 4259–4270.
[21] J.M. Tarbell, Shear stress and the endothelial transport barrier, Cardiovasc. Res. 87 (2010) 320–330.
[22] Y. Matsumoto, T. Nomoto, H. Cabral, Y. Matsumoto, S. Watanabe, R.J. Christie, et al., Direct and instantaneous observation of intravenously injected substances using intravital confocal micro-videography, Biomed. Opt. Express 1 (2010) 1209–1216.
[23] Y. Komarova, A.B. Malik, Regulation of endothelial permeability via paracellular and transcellular transport pathways, Annu. Rev. Physiol. 72 (2010) 463–493.
[24] P.N. Yaron, B.D. Holt, P.A. Short, M. Lösche, M.F. Islam, K.N. Dahl, Single wall carbon nanotubes enter cells by endocytosis and not membrane penetration, J. Nanobiotechnol. 9 (2011) 45.
[25] L. DeMaio, J.M. Tarbell, R.C. Scaduto, T.W. Gardner, D.A. Antonetti, A transmural pressure gradient induces mechanical and biological adaptive responses in endothelial cells, Am. J. Physiol. Heart Circ. Physiol. 286 (2004) H731–H741.